

Journal of Biomedical Optics

BiomedicalOptics.SPIEDigitalLibrary.org

Time-resolved fluorescence spectroscopy and ultrasound backscatter microscopy for nondestructive evaluation of vascular grafts

Hussain Fatakdawala
Leigh G. Griffiths
Sterling Humphrey
Laura Marcu

Time-resolved fluorescence spectroscopy and ultrasound backscatter microscopy for non-destructive evaluation of vascular grafts

Hussain Fatakdwala,^a Leigh G. Griffiths,^b Sterling Humphrey,^c and Laura Marcu^{a,*}

^aUniversity of California Davis, Department of Biomedical Engineering, 451 East Health Sciences Drive, Davis, California 95616, United States

^bUniversity of California Davis, Department of Medicine and Epidemiology, VM2 Building, Davis, California 95618, United States

^cUniversity of California Davis, Department of Surgery, 2221 Stockton Boulevard, Sacramento, California 95817, United States

Abstract. Quantitative and qualitative evaluations of structure and composition are important in monitoring development of engineered vascular tissue both *in vitro* and *in vivo*. Destructive techniques are an obstacle for performing time-lapse analyses from a single sample or animal. This study demonstrates the ability of time-resolved fluorescence spectroscopy (TRFS) and ultrasound backscatter microscopy (UBM), as nondestructive and synergistic techniques, for compositional and morphological analyses of tissue grafts, respectively. UBM images and integrated backscatter coefficients demonstrate the ability to visualize and quantify postimplantation changes in vascular graft biomaterials such as loss of the external elastic lamina and intimal/medial thickening over the grafted region as well as graft integration with the surrounding tissue. TRFS results show significant changes in spectra, average lifetime, and fluorescence decay parameters owing to changes in collagen, elastin, and cellular content between normal and grafted tissue regions. These results lay the foundation for the application of a catheter-based technique for *in vivo* evaluation of vascular grafts using TRFS and UBM. © 2014 Society of Photo-Optical Instrumentation Engineers (SPIE) [DOI: 10.1117/1.JBO.19.8.080503]

Keywords: optical spectroscopy; ultrasound; time-resolved fluorescence; vascular; grafts.

Paper 140327LR received May 31, 2014; revised manuscript received Jul. 28, 2014; accepted for publication Aug. 1, 2014; published online Aug. 22, 2014.

The translation of tissue-engineered products into a clinical setting or a commercial market requires cost effective and robust monitoring of tissue constructs during development both *in vitro* and *in vivo*.¹ Traditional destructive methods (e.g., assays and mechanical testing) are a clear impediment to such translation

as dynamic or time-lapse measurements—important for long-term cell/tissue studies, are difficult to perform using such methods due to their inefficiency in time and cost. Thus, there is a clear need for nondestructive methods that allow time-lapse evaluation of engineered tissue constructs during development, both *in vitro* and *in vivo*, without sacrificing the sample or animal.

Engineering of vascular grafts is an important area of research aimed at enabling vascular reconstruction in patients with atherosclerosis, surgical excision, and trauma-related vascular problems. Such grafts can serve as an alternative when autologous saphenous vein or mammary artery is not available or of inadequate length.² A percutaneous technique capable of time-lapse characterization of vascular grafts *in vivo* without having to sacrifice the experimental animal would be extremely useful. A bimodal imaging catheter³ can enable such an investigation.

Here, we report results from a pilot study aimed at evaluating *ex vivo* vascular grafts using two intravascular compatible modalities, namely time-resolved fluorescence spectroscopy (TRFS) and ultrasound backscatter microscopy (UBM). TRFS allows detection of compositional changes in tissue such as alteration in collagen, elastin, and cellular content, whereas UBM allows visualization of structure and morphology of arterial vessels. Our prior work has shown that TRFS and UBM can be integrated into a compact rotational catheter³ for characterization of atherosclerotic lesions.⁴ The overall goal of this study is to test whether these modalities can complement each other in inferring compositional and structural information from explanted vascular grafts. The results from this study will help define the framework for future *in vivo* vessel graft characterization studies using a catheter-based imaging technique.³

Vascular grafts can be composed of synthetic materials or derived from processed native tissue or cell seeded scaffolds. We studied Hemashield®, a synthetic graft (Dacron®) impregnated with collagen, and CorMatrix®, a porcine small intestinal submucosal extracellular matrix (ECM) graft, to assess the morphological and compositional differences between a synthetic and biopolymer graft using TRFS and UBM.

1 Methods

Vascular patch materials (CorMatrix® or Hemashield®) were implanted as a 2 × 0.6 cm patch in a porcine carotid arteriotomy model. A 2-cm longitudinal arteriotomy was made on the anterior surface of the right carotid artery and repaired using a patch (either CorMatrix® or Hemashield®) sutured in place with running suture of 6-0 Prolene® (Ethicon, Inc., Somerville, New Jersey). Hemostasis was achieved using manual pressure, additional sutures, and a topical hemostatic agent (Surgicel®, Ethicon, Inc.).

Carotid explants from three pigs (one with Hemashield® and two with CorMatrix® vascular grafts) were available for this pilot study. The vessels (~1.5 to 2 cm segments) were harvested (90 days postimplantation) and incised longitudinally to expose the luminal surface for TRFS and UBM measurements (<4 h postharvest).

TRFS and UBM measurements of a given tissue region of interest (1-mm diameter for TRFS) were performed using a prototype system⁵ developed in our laboratory. Point TRFS measurements (excitation: 337 nm, 2 μJ/pulse, 800-ps pulse width, emission: 360 to 500 nm, 5-nm steps) were performed

*Address all correspondence to: Laura Marcu, E-mail: lmarcu@ucdavis.edu

in triplicates for two different luminal surface locations in regions containing the graft and regions of normal nongrafted vessel (identified by the presence of sutures). Fluorescence decay values (average lifetime, τ and second-order Laguerre coefficient, LC-2) were estimated using a constrained least-square deconvolution with Laguerre expansion technique.⁶ UBM (40 MHz, single-element transducer, resolution—30 μm , axial; 60 μm , lateral) imaging scans were performed across regions containing the graft as well as regions without the graft for comparison. UBM data were analyzed as described in our previous work.⁷

Histologic sections (formalin fixed) were obtained from regions of the sample with and without grafts and stained with hematoxylin and eosin (for visualization of morphology), Verhoeff van Gieson (VVG, for the visualizing elastic fibers), and Masson's trichrome (for visualizing the collagen content in intima/media layers).

Statistical significance between measurements was determined by student's *t*-test ($p < 0.05$).

2 Results and Discussion

The sample shown in Fig. 1 depicts the TRFS and UBM results from synthetic vascular graft material (Hemashield®). The spatial location of the graft is observed in the UBM cross-sectional image [arrow C, Fig. 1(d)] and confirmed in histology. The region between the internal and external elastic laminae [arrow D, Fig. 1(f)] appears hypoechoic in a normal vessel due to lower collagen content and higher elastin content. The graft appeared to not integrate well with the surrounding tissue as demonstrated by the hypoechoic regions seen in the UBM image corresponding to lack of collagen fibers in and around the graft. These regions are observed as collagen poor areas in the graft in histology [Fig. 1(e)]. The histologic results also show that the intimal/medial surface above the graft is composed primarily of collagen [arrow A, Fig. 1], and lacks elastic fibers and the external elastic lamina when compared with normal tissue [Fig. 1(e), arrow B and Fig. 1(g), arrow D]. These

features are also observed by UBM as loss of visible layered structure over the grafted region [arrow A, Fig. 1(d)] and discontinued external elastic lamina [arrow B, Fig. 1(d)]. TRFS results show narrowing of the fluorescence emission spectra and slight blue-shifted peak [Fig. 1(a)] for the grafted tissue region when compared with the normal tissue region. These changes in fluorescence properties can be attributed to the increase in collagen content and lack of elastin fibers over the grafted region. Collagen is known to have a narrower, blue-shifted emission spectra and higher τ value when compared with elastin.⁸ Consequently, the τ values are higher ($p < 0.05$) over the grafted region for shorter wavelengths (6.27 \pm 0.09 ns, 395 to 410 nm band) when compared with normal tissue (6.01 \pm 0.08 ns, 395 to 410 nm band). The trend reverses for higher wavelengths owing to higher fluorescence signal contribution from cellular components and elastin in normal tissue. LC-2 values reflect the changes in fluorescence decay dynamics. These values (465 to 500 nm band) were higher ($p < 0.04$) for the grafted region (-0.011 ± 0.008) as compared with the normal regions (-0.024 ± 0.011). LC-2 values had an opposite trend for shorter wavelengths but were not significantly different between grafted and normal regions. Nonetheless, the change in composition in the vessel from the graft is made evident by TRFS results. Integrated backscatter coefficients (IBC) correlate to tissue stiffness, and hence increase in collagen content will cause an increase in these coefficient values (-13.98 ± 4.04 dB for normal regions and -9.45 ± 3.48 dB for grafted regions, Fig. 1).

Figure 2 depicts the results from the porcine small intestinal submucosal ECM-based graft (CorMatrix®) that appears to integrate more completely with the surrounding tissue although, based on histology, the lack of elastin fibers is still evident [arrow A, Fig. 2(e)]. The normal tissue regions [Fig. 2(g)] have relatively higher elastin content in the medial layer that generates a stark change in chemical composition (elastin) between the normal and grafted regions. The high elastin content in normal vessel is characteristic of large elastic arteries such as the proximal portions of the carotid artery. Higher elastin

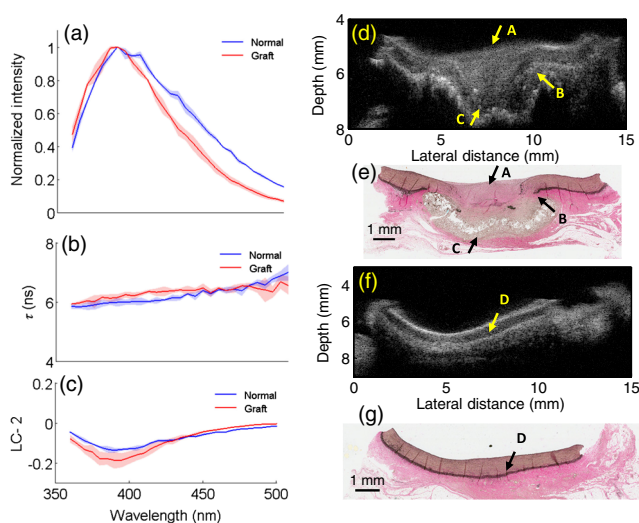


Fig. 1 Pig carotid sample (1) with Hemashield® graft. TRFS results: (a) fluorescence spectra, (b) τ , and (c) LC-2 values from normal and grafted tissue areas. Standard deviation (SD) is shown as shaded areas. UBM image of vessel showing (d) grafted (arrow C) and (f) normal area with corresponding registered Verhoeff van Gieson (VVG)-stained histology section in (e) and (g), respectively.

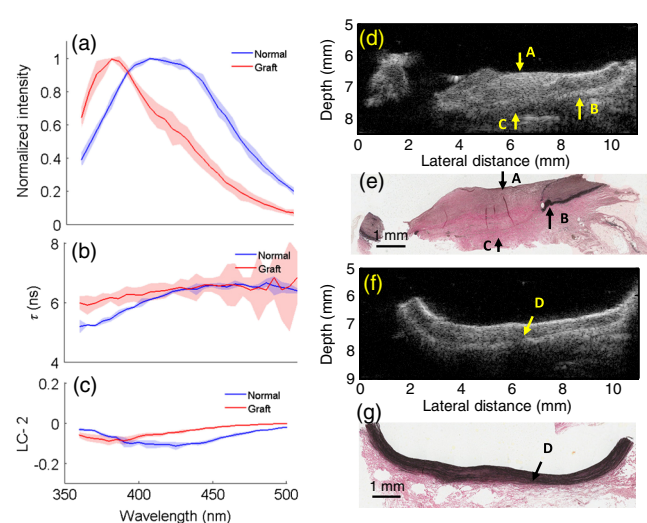


Fig. 2 Pig carotid sample (2) with CorMatrix® graft. TRFS results: (a) fluorescence spectra, (b) τ , and (c) LC-2 values from normal and grafted tissue areas. SD is shown as shaded areas. UBM image of vessel showing (d) grafted (arrow C) and (f) normal area with corresponding registered VVG-stained histology section in (e) and (g), respectively.

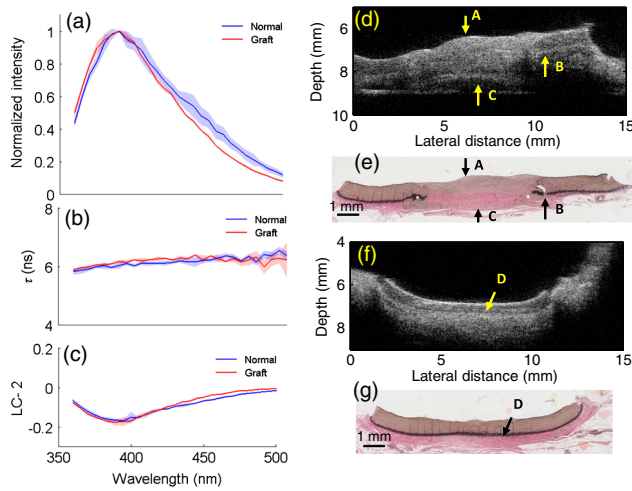


Fig. 3 Pig carotid sample (3) with CorMatrix® graft. TRFS results: (a) fluorescence spectra, (b) τ , and (c) LC-2 values from normal and grafted tissue areas. SD is shown as shaded areas. UBM image of vessel showing (d) grafted (arrow C) and (f) normal area with corresponding registered VVG-stained histology section in (e) and (g), respectively.

content appears to contribute to a large spectral shift in peaks between normal and grafted regions [Fig. 2(a)]. The relatively lower elastin content in the normal regions surrounding the graft may be because of graft-induced remodeling. The τ values at shorter wavelengths (370 to 380 nm band) are higher ($p < 0.02$) over the grafted region (6.08 ± 0.18 ns) when compared with normal tissue (5.35 ± 0.12 ns). LC-2 values (410 to 500 nm band) were higher ($p < 0.01$) for the grafted region (-0.025 ± 0.019) when compared with the normal regions (-0.073 ± 0.034). IBC values were higher for the grafted regions (-3.45 ± 2.52 dB) when compared with the normal regions (-14.01 ± 4.67 dB).

Figure 3 depicts the results from another CorMatrix® vascular graft. Similar to the previous samples, loss of elastic fibers in the grafted regions is evident in histology [Fig. 3(e)]. UBM cross-sectional image allows visualizing the presence of the graft [arrow C, Fig. 3(d)] and also the loss of the external elastic lamina [arrow B, Fig. 3(d)]. This sample, however, showed low elastin content (significantly fewer elastic fibers in media) in the normal tissue areas as well [Fig. 3(g)]. TRFS results between normal and grafted regions were not significantly different unlike the sample shown in Fig. 2. The trends in spectra, τ , and LC-2 values, however, were similar to the results from the sample in Fig. 2. The τ values (395 to 410 nm) from the grafted region (6.19 ± 0.07 ns) were higher ($p < 0.5$) than normal tissue (6.09 ± 0.07 ns). The LC-2 values (440 to 460 nm) were higher ($p < 0.02$) for grafted regions (-0.050 ± 0.013) when compared with normal regions (-0.070 ± 0.012). IBC values for normal and grafted regions were -9.55 ± 5.23 dB and -6.27 ± 3.77 dB, respectively.

These results show the ability of TRFS to track compositional changes in grafted vessels (collagen and elastin contents) and UBM to image graft integration with surrounding tissue along with related morphological changes (loss of elastic lamina and intimal/medial thickening over the grafted region). Interestingly, despite variations in the compositional features between the two CorMatrix® vascular grafts (Figs. 2 and 3), as confirmed by histology and depicted by TRFS, current data demonstrate that these grafts integrate better with the surrounding tissue when compared with the Hemashield® graft (Fig. 1). This integration can be nondestructively observed using UBM.

3 Conclusions

Results from this pilot study demonstrate that TRFS and UBM together allow for nondestructive evaluation of vascular tissue graft composition and morphology, respectively. UBM allows visualizing the spatial location of the graft and its integration with surrounding tissue. It also enables visualizing the intimal/medial thickening and loss of the external elastic lamina over the grafted region. These observations are complemented with compositional information about collagen and elastin contents via changes in fluorescence spectra, τ , and LC-2 values. This work lays the foundation for the future use of a bimodal catheter combining both techniques for nondestructive evaluation of vascular grafts *in vivo*.

Acknowledgments

This work was supported by NIH Grants R01-HL67377 and 5T32EB003827.

References

1. M. L. Mather, S. P. Morgan, and J. A. Crowe, "Meeting the needs of monitoring in tissue engineering," *Regener. Med.* **2**(2), 145–160 (2007).
2. M. R. Hoenig et al., "Tissue-engineered blood vessels: alternative to autologous grafts?," *Arterioscler., Thromb., Vasc. Biol.* **25**(6), 1128–1134 (2005).
3. D. Ma et al., "Rotational multispectral fluorescence lifetime imaging and intravascular ultrasound: bimodal system for intravascular applications," *J. Biomed. Opt.* **19**(6), 066004 (2014).
4. Y. Sun et al., "Multimodal characterization of compositional, structural and functional features of human atherosclerotic plaques," *Biomed. Opt. Express* **2**(8), 2288–2298 (2011).
5. Y. Sun et al., "Development of a dual-modal tissue diagnostic system combining time-resolved fluorescence spectroscopy and ultrasonic backscatter microscopy," *Rev. Sci. Instrum.* **80**(6), 065104 (2009).
6. J. Liu et al., "A novel method for fast and robust estimation of fluorescence decay dynamics using constrained least-squares deconvolution with Laguerre expansion," *Phys. Med. Biol.* **57**(4), 843–865 (2012).
7. H. Fatakdawala et al., "Multimodal in vivo imaging of oral cancer using fluorescence lifetime, photoacoustic and ultrasound techniques," *Biomed. Opt. Express* **4**(9), 1724–1741 (2013).
8. M. Y. Berezin and S. Achilefu, "Fluorescence lifetime measurements and biological imaging," *Chem. Rev.* **110**(5), 2641–2684 (2010).